Science of the Total Environment 837 (2022) 155464

Contents lists available at ScienceDirect

Science of the Total Environment

journal homepage: www.elsevier.com/locate/scitotenv

Short communication

Detection of excited triplet species from photolysis of carbonyls: Direct evidence for single oxygen formation in atmospheric environment

Jiangyao Chen [a,b,*], Xu-nuo Miao [a], Taicheng An [a,b]

[a] Guangdong Key Laboratory of Environmental Catalysis and Health Risk Control, Guangdong Technology Research Center for Photocatalytic Technology Integration and Equipment Engineering, Institute of Environmental Health and Pollution Control, Guangdong University of Technology, Guangzhou 510006, China

[b] Guangzhou Key Laboratory of Environmental Catalysis and Pollution Control, Guangdong-Hong Kong-Macao Joint Laboratory for Contaminants Exposure and Health, School of Environmental Science and Engineering, Guangdong University of Technology, Guangzhou 510006, China

HIGHLIGHTS

- Dicarbonyl displayed higher $^1O_2$ production than monocarbonyl.
- $^3PA^*$ formation was confirmed by laser flash photolysis technique for the first time.
- Added inorganic salt or increased solution pH decreased $^3PA^*$ and $[^1O_2]_{SS}$ of PA.
- High excited triplet species in photolysis of MG and DMA enhanced $[^1O_2]_{SS}$.
- Direct evidence for $^1O_2$ formation in atmospheric environment was obtained.

GRAPHICAL ABSTRACT

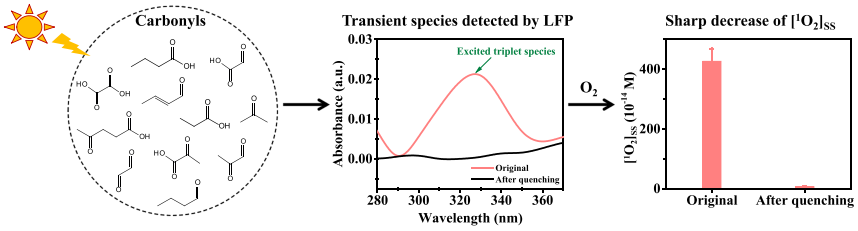

ARTICLE INFO

Editor: Pingqing Fu

Keywords:
Carbonyls
Reactive oxygen species
Transient substances
Laser flash photolysis
Quenching experiment

ABSTRACT

Excited triplet species play an important role in the photolytic formation of $^1O_2$ from carbonyls, but the related mechanism is still uncertain, due to lack of direct evidence. In this study, steady-state and transient photolysis of eleven carbonyls to produce $^1O_2$ was investigated. Dicarbonyl displayed greater $^1O_2$ production ability than monocarbonyl, while dicarbonyl containing both ketone and carboxyl groups connected by CC bond (i.e., pyruvic acid (PA)) showed the highest $^1O_2$ steady-state concentration ($[^1O_2]_{SS}$). For the first time, the production of $^3PA^*$ from PA with narrow energy gap was confirmed by laser flash photolysis technique and the second-order decay rate constant of $^3PA^*$ was $2.78 \times 10^7\ M^{-1}\ s^{-1}$. Quenching results verified the dominant contribution of $^3PA^*$ to $^1O_2$ production from PA. Addition of inorganic salt or increase in solution pH showed negligible effect on $^3PA^*$, but significantly decreased the $[^1O_2]_{SS}$ of PA by up to two orders of magnitude, due to reduction of hydrate content. Photolysis of methylglyoxal and dimethylamine mixture led to higher content of excited triplet species at pH ≈ 11 and remarkably enhanced $[^1O_2]_{SS}$, which was 2.3 times of that from PA and dimethylamine mixture. These findings provide direct evidence for the contribution of transient species from carbonyls or their product to $^1O_2$ formation in atmospheric environment.

1. Introduction

Carbonyls are a group of highly reactive and toxic pollutants in the atmosphere, threatening air quality and human health. The International Agency for Research on Cancer has classified several carbonyls as toxic air pollutants and even human carcinogens (Liu et al., 2020; Weng et al., 2009). Moreover, carbonyls not only form secondary organic aerosols (Sareen et al., 2010; Schwier et al., 2010; Woo et al., 2013; Knote et al., 2014; Rincon et al., 2010; Rincon et al., 2009) and other atmospheric polymerized pollutants (Rossignol et al., 2014; Fu et al., 2015; Guzman et al., 2006a), but also significantly contribute to production of ozone (Duan et al., 2008; Yuan et al., 2012; Wang et al., 2018; Shen et al., 2021), causing secondary pollution. In addition, carbonyls can photochemically produce reactive oxygen species (ROS) (Anastasio et al., 1997; Rohrer et al., 2014;

* Corresponding author at: Guangdong Key Laboratory of Environmental Catalysis and Health Risk Control, Guangdong Technology Research Center for Photocatalytic Technology Integration and Equipment Engineering, Institute of Environmental Health and Pollution Control, Guangdong University of Technology, Guangzhou 510006, China.
E-mail address: chenjiangyao@gdut.edu.cn (J. Chen).

http://dx.doi.org/10.1016/j.scitotenv.2022.155464
Received 18 February 2022; Received in revised form 8 April 2022; Accepted 19 April 2022
Available online 1 May 2022

Yang et al., 2018; Guzman et al., 2006b), which further react with the carbonyls or other compounds to generate complex intermediates (Zhang et al., 2021; Xia et al., 2018; Eugene and Guzman, 2019a; Guzman and Eugene, 2021). While the harmful effect of carbonyls on human body and their pollution to atmospheric environment have received considerable attention from researchers, studies on photochemical production of ROS from carbonyls and potential implications for atmospheric chemistry are recently becoming widespread.

Available studies mostly focus on the photochemical production of free radicals (e.g., $^{\bullet}OH$, $^{\bullet}HO_2$, $^{\bullet}RO_2$) from organics (Rohrer et al., 2014; Yang et al., 2018; Tan et al., 2017). Besides these radicals, $^1O_2$ is inevitably produced during photolysis of organics because it is easily formed through the transfer of energy from excited organic matter to O_2 (Ogilby, 2010). Till now, various organics-containing environmental substances, such as rainwater (Albinet et al., 2010), fogwater (Kaur and Anastasio, 2017), particulate matter (Manfrin et al., 2019), road dust (Cote et al., 2018), green leaf volatiles (Richards-Henderson et al., 2015), biochar (Fu et al., 2016), soot (Li et al., 2019), secondary organic aerosol (Manfrin et al., 2019) and wastewater organic matter (Mostafa and Rosario-Ortiz, 2013), have been confirmed to produce $^1O_2$ after photolysis treatment. The resulting $^1O_2$ not only affects the fate of aerosol tracers, pollutants within aerosols and toxins (Kaur and Anastasio, 2017; Manfrin et al., 2019; Cote et al., 2018; Richards-Henderson et al., 2015), but also reacts with proteins, DNA and biomolecules, initiating irreversible damage to cells (Briviba et al., 1997). All these studies suggest that it is essential to deeply understand the production mechanism of $^1O_2$ from organics to prevent its negative effect on environmental quality and human health. Unfortunately, the above studies did not attempt to reveal the mechanism, probably due to the complex composition of these substances. Recently, mechanism involving excited state species has been proposed to play a significant role in $^1O_2$ production from pure organics (Eugene and Guzman, 2019b; Lin et al., 2021). However, there is still no direct observation of the excited state species produced from photolysis of carbonyls.

In this study, eleven carbonyls with different structures were selected as model compounds to investigate their ability to photolytically produce $^1O_2$. Then, laser flash photolysis technique was applied to directly identify the excited state species. Quenching experiments were also performed in steady state and transient experiments to further verify the contribution of excited state species to the formation of $^1O_2$. Energy gap of carbonyl molecules was calculated to illustrate their ability to be excited. Finally, the variations of excited state species and $^1O_2$ steady-state concentration were compared with addition of inorganic salt and organic amine as well as change in solution pH to reveal whether the contribution of excited state species to $^1O_2$ formation from carbonyls was also applicable under complex environments.

2. Materials and methods

2.1. Experiment description

Furfuryl alcohol (FFA) and eleven carbonyls (Table S1) were successively dissolved in 20 mL of distilled water to obtain solutions with initial concentrations of 100 μM and 5 mM, respectively. A Xe lamp (300 W, PLS-SXE300+) vertically irradiated the solution from the top to trigger $^1O_2$ formation reaction (Figs. S1 and S2). The effects of inorganic salt, solution pH and organic amine on $^1O_2$ formation from pyruvic acid (PA) and methylglyoxal (MG) were also investigated (see detailed description in Supporting Information (SI)).

2.2. Singlet oxygen determination

FFA was used to determine $^1O_2$ and quantified by high performance liquid chromatography (HPLC) with C18 column (see detailed description in SI). Control experiment showed negligible photolysis of FFA to $^1O_2$. The steady-state concentration and quantum yield of $^1O_2$ ($[^1O_2]_{SS}$ and Φ_{1O2}) were calculated via the equations given in SI.

2.3. Transient and steady-state product analysis

A laser flash photolysis spectrometer (LKS80) equipped with Nd:YAG laser was used to identify transient species. The wavelength and pulse interval of the laser were 266 nm and 5 ns, and the energy of each pulse was 10–15 mJ. The light source was a Xe lamp. The excitation and detection beams passed through a slit (1 × 10 mm) perpendicularly, and irradiated the quartz reaction cuvette (10 × 10 × 40 mm). The transmitted light entered a monochromator equipped with a R955 photomultiplier and the output signal of the digital oscilloscope (HP 54510 B) was recorded for analysis.

Triethanolamine (TEOA, 5 mM) and 2,4,6-trimethylphenol (TMP, 2 mM) were used as quenchers for excited triplet species, and monitored by HPLC. Ultra-performance liquid chromatography-quadrupole-orbitrap high resolution mass spectrometry (UPLC-Q-Orbitrap HRMS, Q Exactive) was used for steady-state product identification before and after quenching experiments. Detailed description of the analysis processes is given in SI.

2.4. Theoretical calculations

Calculations were performed using the Gaussian 09 program, and the m062x/6-311 g** basis set was used for geometrical optimizations for all atom, simulation of systems in solution using the self-consistent reaction field (SCRF) method. Setting water as solvent, SMD model for solventization effect can get optimized results. Then Multiwfn (Lu and Chen, 2012) and VMD (Humphrey et al., 1996) were used to draw HOMO and LUMO orbitals. Energies of the highest occupied molecular orbitals (E_{HOMO}) and lowest unoccupied molecular orbitals (E_{LUMO}) were obtained to describe the thermodynamic properties of carbonyls.

3. Results and discussion

3.1. Single oxygen formation from photolysis of carbonyls

Photolysis of eleven carbonyls (5 mM) for 60 min under full spectrum of Xe lamp resulted in $[^1O_2]_{SS}$ ranging from $(0.2 \pm 0.1) \times 10^{-14}$ to $(4.3 \pm 0.4) \times 10^{-12}$ M (Fig. 1). The 5 mM of carbonyls was selected in this study, due to that previous study estimated that acidic urban aerosols contained ≥5 mM PA (Guzman et al., 2006c; Eugene and Guzman, 2017a). The obtained $[^1O_2]_{SS}$ was of similar order of magnitude compared with that from atmospheric particulate organic matter and black carbon (Fu et al., 2016; Li et al., 2019; Appiani and McNeill, 2015), suggesting the important contribution of atmospheric carbonyls to $^1O_2$ formation. The $[^1O_2]_{SS}$ values of acetone (ACE), n-butyraldehyde (NB), butyric acid (BA), propionic acid (PPA) and crotonaldehyde (CRO) were close, ranging from

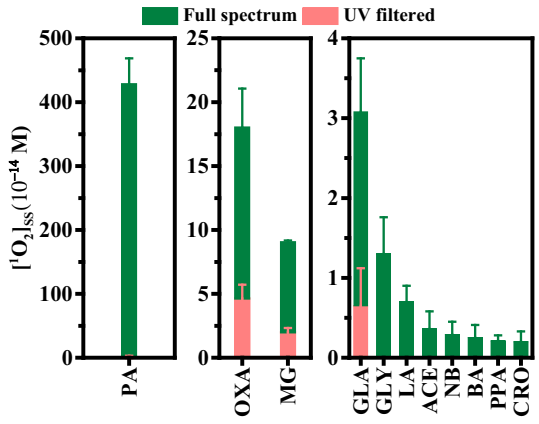

Fig. 1. $^1O_2$ steady-state concentrations of 5 mM carbonyls dissolved in water under Xe lamp irradiation with or without UV filter. More information is shown in Table S1.

$(0.2 \pm 0.1) \times 10^{-14}$ to $(0.4 \pm 0.2) \times 10^{-14}$ M. Higher $[^1O_2]_{SS}$ was obtained from glyoxylic acid (GLA, $(2.4 \pm 0.7) \times 10^{-14}$ M), glyoxal (GLY, $(1.3 \pm 0.5) \times 10^{-14}$ M) and levulinic acid (LA, $(0.7 \pm 0.2) \times 10^{-14}$ M). Dicarbonyl showed greater production ability of $^1O_2$ than monocarbonyl. Oxalic acid (OXA) and MG are also dicarbonyls, which displayed high $[^1O_2]_{SS}$ ($(1.3 \pm 0.3) \times 10^{-13}$ and $(0.7 \pm 0.2) \times 10^{-13}$ M), confirming the above conclusion. The $[^1O_2]_{SS}$ from OXA was found more than ten times of that from GLY, further revealing higher production of $^1O_2$ from dicarbonyl with carboxyl group relative to aldehyde group.

The $[^1O_2]_{SS}$ and Φ_{1O2} of another dicarbonyl, PA, were $(4.3 \pm 0.4) \times 10^{-12}$ M and $(15.4 \pm 1.5) \times 10^{-3}$ (Table S1), at least one order of magnitude higher compared to other dicarbonyls. Eugene et al. provided a direct quantitative comparison of the $^1O_2$ production from PA recently (Eugene and Guzman, 2019b). However, they did not study the effect of the structure of carbonyl on $^1O_2$ production. The synergetic effect of ketone and carboxyl groups of PA may lead to remarkably enhanced production of $^1O_2$. However, very low $[^1O_2]_{SS}$ was produced from LA, which also contains ketone and carboxyl groups. Further comparison revealed that the ketone and carboxyl groups in PA are connected by CC bond, while those in LA are linked via C-C-C-C bond. Shorter bond linkage between two carbonyl groups favors $^1O_2$ formation. The carbonyl groups in OXA, MG, GLA and GLY with relatively high $[^1O_2]_{SS}$ are also connected by CC bond, supporting the above conclusion. To sum up, dicarbonyl displayed greater photolytic $^1O_2$ production ability than monocarbonyl, while dicarbonyl containing CC connected ketone and carboxyl groups led to the highest $[^1O_2]_{SS}$.

Fu et al. proposed that carbonyl-containing structures other than aromatic ketones were involved in $^1O_2$ formation (Fu et al., 2016). In this study, ACE displayed the highest $[^1O_2]_{SS}$ among five monocarbonyls, suggesting that the ketone group contributes to $^1O_2$ production. When ketone group coexisted with carboxyl group, the resulting compound (e.g., PA) led to higher $[^1O_2]_{SS}$, further highlighting the contribution of ketone group to $^1O_2$ production. Recently, Wang et al. found that compared with -COOH, the presence of $-OCH_3$ and quinone in the appropriate position was more favorable for the production of $^1O_2$ mediated by aromatic hydrocarbons (Wang et al., 2020). Although $[^1O_2]_{SS}$ values from BA and PPA (containing -COOH) were also very low, ranking second and third to last in this study, PA and LA were more conducive to the formation of $^1O_2$ when -COOH coexisted with ketone group.

The n-π^* transition occurs when carbonyl structure is excited by UV light (Sidman, 1958), possibly contributing to $^1O_2$ formation. Based on the fact, it was explored whether visible light also participates in the formation of $^1O_2$. No $^1O_2$ was detected from GLY and six monocarbonyl compounds after filtering UV (Fig. 1), although the light intensity changed very little (from 23.4 to 23.1 mW cm^{-2}). Under the same conditions, about $(0.7 \pm 0.5) \times 10^{-14}$, $(1.1 \pm 2.0) \times 10^{-14}$, $(2.0 \pm 0.3) \times 10^{-14}$ and $(4.6 \pm 1.1) \times 10^{-14}$ M of $[^1O_2]_{SS}$ were obtained from GLA, PA, MG and OXA, accounting for 26.7%, 0.25%, 28.3% and 34.6% of total $[^1O_2]_{SS}$, respectively. Clearly, the visible light component of the lamp contributed significantly to $^1O_2$ formation of GLA, MG and OXA, due to their visible light absorption (Fig. S3).

3.2. Steady-state and transient products from photolysis of carbonyls

PA was selected as a model to investigate the photolysis products of carbonyls. After 4 h reaction, three steady-state products with *m/z* of 175.06, 177.04 and 219.05 were detected (Fig. S4). Based on the information of $^1O_2$ and photolysis products in this study as well as previous studies (Guzman et al., 2006a; Eugene and Guzman, 2019b; Mekic et al., 2019a; Eugene and Guzman, 2017b), it was deduced that the excited triplet species (e.g., ^{3}PA*) significantly determined the production of both $^1O_2$ and the three intermediates from PA (Fig. S5). To verify this hypothesis, two common quenchers of excited triplet species, TMP (Bodhipaksha et al., 2015; Ossola et al., 2019; Zhou et al., 2019) and TEOA (Gao et al., 2020), were separately added into the photolysis reaction of PA. The proportion of $[^1O_2]_{SS}$ correspondingly decreased by 98.2% and 94.1% (Fig. S6a), while the content of the three products was reduced by at least one order of magnitude (Fig. S6b). These results indicate the formation of ^{3}PA* from photochemical reaction of PA as well as the decisive role of ^{3}PA* in producing $^1O_2$ and other products.

Fig. 2a further compares the photolysis kinetic curves of TMP in the presence of PA or MG. The decay points of TMP with or without MG almost overlapped, resulting in similar decay rate of $(1.9 \pm 0.7) \times 10^{-3}$ min^{-1} for TMP. This result suggests either negligible formation of excited triplet species during photolysis of MG or very slow reaction rate of the excited triplet species with TMP. During photolysis of TMP with PA, a faster decay rate ($(6.0 \pm 0.3) \times 10^{-3}$ min^{-1}) for TMP was achieved, again revealing the production of ^{3}PA* from photolysis of PA. Evidently, PA can produce ^{3}PA* after irradiation by Xe lamp and further convert dissolved oxygen to $^1O_2$ and form other polymeric products.

Theoretically, ^{3}PA* is from ^{1}PA*. However, due to the lack of direct observation of ^{1}PA* and ^{3}PA*, a firm transformation process between them cannot be obtained. To address this issue, laser flash photolysis technique was applied to identify the transient species. Compared with the control spectrum from pure water, an intense peak at around 330 nm was observed in the spectrum of PA (Fig. 2b), which can be ascribed to the absorption of its transient species. The peak of transient species was stable for 0.1 μs and then decreased rapidly. Unlike radicals, excited triplet species easily react with O_2 to accelerate self-decay (Gawargy et al., 2022; Frimmel et al., 1987). Much stronger absorption peak of transient species with longer self-decay time was observed upon photolysis of PA with N_2 instead of O_2 (Fig. S7), suggesting that the transient species was excited triplet species of PA (i.e., ^{3}PA*). Various excited triplet species have been successfully identified from different organics by laser flash photolysis spectrometer (An et al., 2010; Fang et al., 2013; Yamaji et al., 2016; Fujino et al., 2018), supporting the validity of this method.

In order to further verify whether the transient species was ^{3}PA*, TEOA was added into PA solution. The peak of original transient species completely disappeared after TEOA addition. Thus, the formation of ^{3}PA* from PA was solidly confirmed. By fitting pseudo-first-order exponential decay kinetics at different concentrations of PA (Fig. 2c), the production rate constant of ^{3}PA* from PA photolysis (2.78×10^7 M^{-1} s^{-1}) was obtained (inset in Fig. 2c). Unfortunately, no transient species was observed for the other carbonyls (Fig. S8), although they showed comparable E_{HOMO}-E_{LUMO} gap (e.g., 0.28 eV for MG) as PA (0.30 eV) (Fig. 2d). The possible reason is that the lifetime of transient species from these carbonyls is too short to be detected by the instrument in this study.

3.3. Contribution of excited triplet species to single oxygen formation in complex atmospheric environment

The contribution of excited triplet species to $^1O_2$ production in complex experimental conditions was further investigated. The presence of 1 mM $(NH_4)_2SO_4$, NaCl or Na_2SO_4 decreased the $[^1O_2]_{SS}$ of PA to $(1.6 \pm 0.2) \times 10^{-12}$, $(1.9 \pm 0.1) \times 10^{-12}$ or $(2.3 \pm 0.1) \times 10^{-12}$ M and of MG to $(4.5 \pm 1.8) \times 10^{-14}$, $(4.5 \pm 0.1) \times 10^{-14}$ or $(5.6 \pm 0.1) \times 10^{-14}$ M, respectively (Fig. 3a and b). With the increase in concentration of inorganic salts to 10 and 100 mM, the $[^1O_2]_{SS}$ of PA exhibited an initial increase and then decreased, while that of MG continuously increased. NH_4^+ in $(NH_4)_2SO_4$ showed the greatest impact on variation of $[^1O_2]_{SS}$ for both PA and MG. Previous studies have reported that NH_4^+ is an efficient catalyst for the aldol condensation of carbonyl compounds (Noziere et al., 2010) and the enhanced formation of imidazole via reaction with carbonyls (Lian et al., 2021), partially supporting the present results. The almost unchanged transient species for PA and MG before and after inorganic salt addition indicated that the variation of $[^1O_2]_{SS}$ was related to other species rather than excited triplet species (Fig. S9). On the other hand, increment of pH from 2.71 (or 3.87) to 6.35 (or 6.85) decreased the $[^1O_2]_{SS}$ from $(4.3 \pm 0.1) \times 10^{-12}$ to $(7.0 \pm 0.6) \times 10^{-14}$ for PA (or from $(7.0 \pm 0.4) \times 10^{-14}$ to $(5.0 \pm 1.0) \times 10^{-14}$ for MG) (Fig. 3c). PA and MG in acidic solution preferred the $^1O_2$ production in the presence of DMA (Fig. 3d). Higher $[^1O_2]_{SS}$ was related to high Φ_{1O2} (Tables S2-S5).

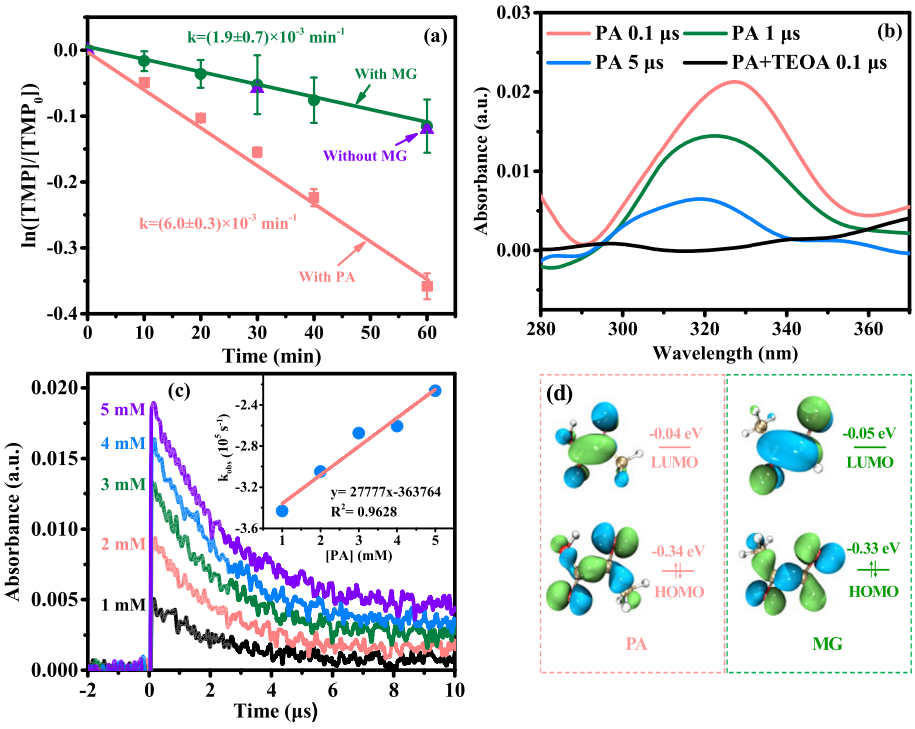

Fig. 2. (a) Photolysis kinetic curves of TMP with or without PA and MG. (b) Time-resolved transient absorption spectra of PA with or without adding TEOA. (c) Decay curve of transient species of PA under different PA concentrations (Inset: the second-order rate constant curve of PA transient species at 330 nm). (d) Simulation results for the orbitals of PA and MG (HOMO: the highest occupied molecular orbitals, LUMO: the lowest unoccupied molecular orbitals).

In comparison, $[^1O_2]_{SS}$ from PA was more significantly affected by pH variation, regardless of the presence of DMA. In water, PA exists as a mixture of the keto form and its hydrate (the geminal diol 2,2-dihydroxypropanoic acid); 5 mM PA contains approximately 50% diol and 50% keto (Mekic et al., 2019b). Previous study suggested that cations (e.g., Na^+, NH_4^+) deprotonate PA, reducing the relative content of diol (Luo et al., 2020). As the pH increased, the ratio of the diol in PA solution also decreased and approached equilibrium when pH > 4 (Rapf et al., 2017). After adding DMA into PA solution, the pH of the mixed solution sharply increased to around 11, accompanied by obviously decreased

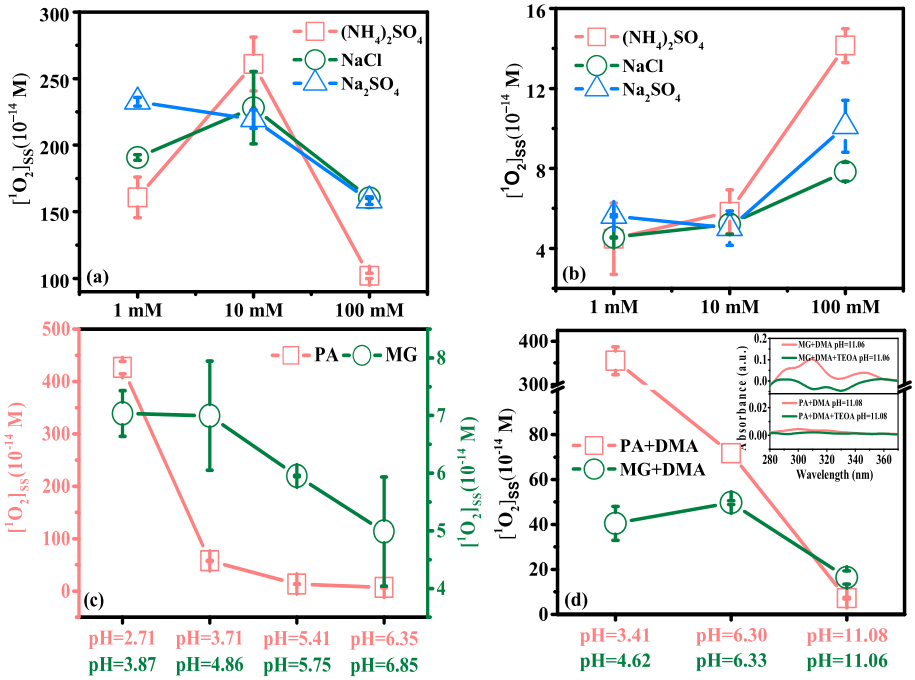

Fig. 3. $^1O_2$ steady-state concentrations of PA and MG in the presence of different inorganic salts (a, b), under different pH (c, pH was adjusted with NaOH), and (d) reacted with DMA for one day under different pH (pH was adjusted with HNO_3. Inset: time-resolved transient absorption spectra in alkaline environment with or without adding TEOA).

$[^1O_2]_{SS}$. These results confirm the strong relationship between $[^1O_2]_{SS}$ and content of diol in PA solution.

Notably, the $[^1O_2]_{SS}$ from mixed MG and DMA was 1.8–5.6 times of that from pure MG, indicating that DMA promoted the $^1O_2$ production of MG. As is known, MG can react with organic amines to produce brown carbon or N-containing oligomers (Powelson et al., 2014; Lin et al., 2015). These formed species not only show excellent light absorption performance, but also have stronger ability to form transient species (Fig. S10), enhancing $^1O_2$ production. This is the first report that observes the significant formation of $^1O_2$ from brown carbon or N-containing oligomers during reaction of carbonyl and organic amines. Interestingly, the $[^1O_2]_{SS}$ obtained from mixed MG and DMA system was 2.3 times of that from mixed PA and DMA system in alkaline environment (Fig. S11). Higher intensity of excited triplet species was observed from the former system (inset in Fig. 3d), again verifying the important contribution of excited triplet species to $^1O_2$ production. However, it is necessary to further investigate the formation mechanism of $^1O_2$ from carbonyls and their products under more complex conditions to comprehensively understand the transformation and fate of carbonyls in real atmospheric environment (Eugene and Guzman, 2019b).

CRediT authorship contribution statement

Jiangyao Chen: Methodology, Formal analysis, Writing – original draft, Conceptualization, Supervision. **Xu-nuo Miao:** Methodology, Formal analysis, Data curation. **Taicheng An:** Writing – review & editing, Conceptualization.

Declaration of competing interest

The authors declare that they have no known competing financial interests or personal relationships that could have appeared to influence the work reported in this paper.

Acknowledgements

This work was financially supported by National Key R&D Program of China (2019YFC0214402), Local Innovative and Research Teams Project of Guangdong Pearl River Talents Program (2017BT01Z032), National Natural Science Foundation of China (42177354, 21777032) and Key-Area Research and Development Program of Guangdong Province (2019B110206002).

Appendix A. Supplementary data

Supplementary data to this article can be found online at https://doi.org/10.1016/j.scitotenv.2022.155464.

References

Albinet, A., Minero, C., Vione, D., 2010. Photochemical generation of reactive species upon irradiation of rainwater: negligible photoactivity of dissolved organic matter. Sci. Total Environ. 408 (16), 3367–3373.

An, T., Yang, H., Li, G., Song, W., Cooper, W.J., Nie, X., 2010. Kinetics and mechanism of advanced oxidation processes (AOPs) in degradation of ciprofloxacin in water. Appl. Catal. B Environ. 94 (3), 288–294.

Anastasio, C., Faust, B.C., Rao, C.J., 1997. Aromatic carbonyl compounds as aqueous-phase photochemical sources of hydrogen peroxide in acidic sulfate aerosols, fogs, and clouds. 1. Non-phenolic methoxybenzaldehydes and methoxyacetophenones with reductants (phenols). Environ. Sci. Technol. 31 (1), 218–232.

Appiani, E., McNeill, K., 2015. Photochemical production of singlet oxygen from particulate organic matter. Environ. Sci. Technol. 49 (6), 3514–3522.

Bodhipaksha, L.C., Sharpless, C.M., Chin, Y.-P., Sander, M., Langston, W.K., MacKay, A.A., 2015. Triplet photochemistry of effluent and natural organic matter in whole water and isolates from effluent-receiving rivers. Environ. Sci. Technol. 49, 3453–3463.

Briviba, K., Klotz, L.O., Sies, H., 1997. Toxic and signaling effects of photochemically or chemically generated singlet oxygen in biological systems. Biol. Chem. 378 (11), 1259–1265.

Cote, C.D., Schneider, S.R., Lyu, M., Gao, S., Gan, L., Holod, A.J., Chou, T.H.H., Styler, S.A., 2018. Photochemical production of singlet oxygen by urban road dust. Environ. Sci. Technol. Lett. 5 (2), 92–97.

Duan, J., Tan, J., Yang, L., Wu, S., Hao, J., 2008. Concentration, sources and ozone formation potential of volatile organic compounds (VOCs) during ozone episode in Beijing. Atmos. Res. 88 (1), 25–35.

Eugene, A.J., Guzman, M.I., 2017. Reactivity of ketyl and acetyl radicals from direct solar actinic photolysis of aqueous pyruvic acid. J. Phys. Chem. A 121, 2924–2935.

Eugene, A.J., Guzman, M.I., 2017. Reactivity of ketyl and acetyl radicals from direct solar actinic photolysis of aqueous pyruvic acid. J. Phys. Chem. A 121 (15), 2924–2935.

Eugene, A.J., Guzman, M.I., 2019. The effects of reactant concentration and air flow rate in the consumption of dissolved O2 during the photochemistry of aqueous pyruvic acid. Molecules 24 (6), 1124.

Eugene, A.J., Guzman, M.I., 2019. Production of singlet oxygen (1O2) during the photochemistry of aqueous pyruvic acid: the effects of pH and photon flux under steady-state O2(aq) concentration. Environ. Sci. Technol. 53 (21), 12425–12432.

Fang, H., Gao, Y., Li, G., An, J., Wong, P.K., Fu, H., Yao, S., Nie, X., An, T., 2013. Advanced oxidation kinetics and mechanism of preservative propylparaben degradation in aqueous suspension of TiO2 and risk assessment of its degradation products. Environ. Sci. Technol. 47 (6), 2704–2712.

Frimmel, F.H., Bauer, H., Putzien, J., Murasecco, P., Braun, A.M., 1987. Laser flash photolysis of dissolved aquatic humic material and the sensitized production of singlet oxygen. Environ. Sci. Technol. 21 (6), 541–545.

Fu, H., Ciuraru, R., Dupart, Y., Passananti, M., Tinel, L., Rossignol, S., Perrier, S., Donaldson, D.J., Chen, J., George, C., 2015. Photosensitized production of atmospherically reactive organic compounds at the air/aqueous interface. J. Am. Chem. Soc. 137 (26), 8348–8351.

Fu, H., Liu, H., Mao, J., Chu, W., Li, Q., Alvarez, P.J., Qu, X., Zhu, D., 2016. Photochemistry of dissolved black carbon released from biochar: reactive oxygen species generation and phototransformation. Environ. Sci. Technol. 50 (3), 1218–1226.

Fujino, S., Yamaji, M., Marciniak, B., 2018. Laser photolysis studies of ω-bond dissociation in aromatic carbonyls of five-membered rings induced by triplet sensitization. J. Photochem. Photobiol.A 365, 39–44.

Gao, Y., Niu, X., Qin, Y., Guo, T., Ji, Y., Li, G., An, T., 2020. Unexpected culprit of increased estrogenic effects: oligomers in the photodegradation of preservative ethylparaben in water. Water Res. 176, 115745.

Gawargy, T.A., Wang, B., Scaiano, J.C., 2022. Unveiling the mechanism for the photochemistry and photodegradation of vanillin. Photochem. Photobiol. 98, 429–433.

Guzman, M.I., Eugene, A.J., 2021. Aqueous photochemistry of 2-oxocarboxylic acids: evidence, mechanisms, and atmospheric impact. Molecules 26 (17), 5278.

Guzman, M.I., Colussi, A.J., Hoffmann, M.R., 2006. Photoinduced oligomerization of aqueous pyruvic acid. J. Phys. Chem. A 110 (10), 3619–3626.

Guzman, M.I., Colussi, A.J., Hoffmann, M.R., 2006. Photogeneration of distant radical pairs in aqueous pyruvic acid glasses. J. Phys. Chem. A 110 (3), 931–935.

Guzman, M.I., Colussi, A.J., Hoffmann, M.R., 2006. Photoinduced oligomerization of aqueous pyruvic acid. J. Phys. Chem. A 110 (10), 3619–3626.

Humphrey, W., Dalke, A., Schulten, K., 1996. VMD: visual molecular dynamics. J. Mol. Graph. 14 (1), 33–38.

Kaur, R., Anastasio, C., 2017. Light absorption and the photoformation of hydroxyl radical and singlet oxygen in fog waters. Atmos. Environ. 164, 387–397.

Knote, C., Hodzic, A., Jimenez, J.L., Volkamer, R., Orlando, J.J., Baidar, S., Brioude, J., Fast, J., Gentner, D.R., Goldstein, A.H., Hayes, P.L., Knighton, W.B., Oetjen, H., Setyan, A., Stark, H., Thalman, R., Tyndall, G., Washenfelder, R., Waxman, E., Zhang, Q., 2014. Simulation of semi-explicit mechanisms of SOA formation from glyoxal in aerosol in a 3-D model. Atmos. Chem. Phys. 14 (12), 6213–6239.

Li, M., Bao, F., Zhang, Y., Sheng, H., Chen, C., Zhao, J., 2019. Photochemical aging of soot in the aqueous phase: release of dissolved black carbon and the formation of (1)O(2). Environ. Sci. Technol. 53 (21), 12311–12319.

Lian, X.F., Zhang, G.H., Yang, Y.X., Lin, Q.H., Fu, Y.Z., Jiang, F., Peng, L., Hu, X.D., Chen, D.H., Wang, X.M., Peng, P.A., Sheng, G.Y., Bi, X.H., 2021. Evidence for the formation of imidazole from carbonyls and reduced nitrogen species at the individual particle level in the ambient atmosphere. Environ. Sci. Technol. Lett. 8 (1), 9–15.

Lin, P., Laskin, J., Nizkorodov, S., Laskin, A., 2015. Revealing brown carbon chromophores produced in reactions of methylglyoxal with ammonium sulfate. Environ. Sci. Technol. 49, 14257–14266.

Lin, J., Dai, Q., Zhao, H., Cao, H., Wang, T., Wang, G., Chen, C., 2021. Photoinduced release of volatile organic compounds from fatty alcohols at the air-water interface: the role of singlet oxygen photosensitized by a carbonyl group. Environ. Sci. Technol. 55 (13), 8683–8690.

Liu, X.K., Liu, R.R., Zhu, B., Ruan, T., Jiang, G.B., 2020. Characterization of carbonyl disinfection by-products during ozonation, chlorination, and chloramination of dissolved organic matters. Environ. Sci. Technol. 54 (4), 2218–2227.

Lu, T., Chen, F., 2012. Multiwfn: a multifunctional wavefunction analyzer. J. Comput. Chem. 33 (5), 580–592.

Luo, M., Shemesh, D., Sullivan, M.N., Alves, M.R., Song, M., Gerber, R.B., Grassian, V.H., 2020. Impact of pH and NaCl and CaCl(2) salts on the speciation and photochemistry of pyruvic acid in the aqueous phase. J. Phys. Chem. A 124 (25), 5071–5080.

Manfrin, A., Nizkorodov, S.A., Malecha, K.T., Getzinger, G.J., McNeill, K., Borduas-Dedekind, N., 2019. Reactive oxygen species production from secondary organic aerosols: the importance of singlet oxygen. Environ. Sci. Technol. 53 (15), 8553–8562.

Mekic, M., Liu, J.P., Zhou, W.T., Loisel, G., Cai, J., He, T., Jiang, B., Yu, Z.Q., Lazarou, Y.G., Li, X., Brigante, M., Vione, D., Gligorovski, S., 2019. Formation of highly oxygenated multifunctional compounds from cross-reactions of carbonyl compounds in the atmospheric aqueous phase. Atmos. Environ. 219, 117046.

Mekic, M., Liu, J., Zhou, W., Loisel, G., Cai, J., He, T., Jiang, B., Yu, Z., Lazarou, Y.G., Li, X., Brigante, M., Vione, D., Gligorovski, S., 2019. Formation of highly oxygenated multifunctional compounds from cross-reactions of carbonyl compounds in the atmospheric aqueous phase. Atmos. Environ. 219, 117046.

Mostafa, S., Rosario-Ortiz, F.L., 2013. Singlet oxygen formation from wastewater organic matter. Environ. Sci. Technol. 47 (15), 8179–8186.

Noziere, B., Dziedzic, P., Cordova, A., 2010. Inorganic ammonium salts and carbonate salts are efficient catalysts for aldol condensation in atmospheric aerosols. Phys. Chem. Chem. Phys. 12 (15), 3864–3872.

Ogilby, P.R., 2010. Singlet oxygen: there is indeed something new under the sun. Chem. Soc. Rev. 39 (8), 3181–3209.

Ossola, R., Schmitt, M., Erickson, P.R., McNeill, K., 2019. Furan carboxamides as model compounds to study the competition between two modes of indirect photochemistry. Environ. Sci. Technol. 53 (16), 9594–9603.

Powelson, M.H., Espelien, B.M., Hawkins, L.N., Galloway, M.M., De Haan, D.O., 2014. Brown carbon formation by aqueous-phase carbonyl compound reactions with amines and ammonium sulfate. Environ. Sci. Technol. 48 (2), 985–993.

Rapf, R.J., Dooley, M.R., Kappes, K., Perkins, R.J., Vaida, V., 2017. pH dependence of the aqueous photochemistry of α-keto acids. J. Phys. Chem. A 121 (44), 8368–8379.

Richards-Henderson, N.K., Pham, A.T., Kirk, B.B., Anastasio, C., 2015. Secondary organic aerosol from aqueous reactions of green leaf volatiles with organic triplet excited states and singlet molecular oxygen. Environ. Sci. Technol. 49 (1), 268–276.

Rincon, A.G., Guzman, M.I., Hoffmann, M.R., Colussi, A.J., 2009. Optical absorptivity versus molecular composition of model organic aerosol matter. J. Phys. Chem. A 113 (39), 10512–10520.

Rincon, A.G., Guzman, M.I., Hoffmann, M.R., Colussi, A.J., 2010. Thermochromism of model organic aerosol matter. J. Phys. Chem. Lett. 1 (1), 368–373.

Rohrer, F., Lu, K., Hofzumahaus, A., Bohn, B., Brauers, T., Chang, C.-C., Fuchs, H., Häseler, R., Holland, F., Hu, M., Kita, K., Kondo, Y., Li, X., Lou, S., Oebel, A., Shao, M., Zeng, L., Zhu, T., Zhang, Y., Wahner, A., 2014. Maximum efficiency in the hydroxyl-radical-based self-cleansing of the troposphere. Nat. Geosci. 7 (8), 559–563.

Rossignol, S., Aregahegn, K.Z., Tinel, L., Fine, L., Nozière, B., George, C., 2014. Glyoxal induced atmospheric photosensitized chemistry leading to organic aerosol growth. Environ. Sci. Technol. 48 (6), 3218–3227.

Sareen, N., Schwier, A.N., Shapiro, E.L., Mitroo, D., McNeill, V.F., 2010. Secondary organic material formed by methylglyoxal in aqueous aerosol mimics. Atmos. Chem. Phys. 10 (3), 997–1016.

Schwier, A.N., Sareen, N., Mitroo, D., Shapiro, E.L., McNeill, V.F., 2010. Glyoxal-methylglyoxal cross-reactions in secondary organic aerosol formation. Environ. Sci. Technol. 44 (16), 6174–6182.

Shen, H., Liu, Y., Zhao, M., Li, J., Zhang, Y., Yang, J., Jiang, Y., Chen, T., Chen, M., Huang, X., Li, C., Guo, D., Sun, X., Xue, L., Wang, W., 2021. Significance of carbonyl compounds to photochemical ozone formation in a coastal city (Shantou) in eastern China. Sci. Total 1Environ. 764, 144031.

Sidman, J.W., 1958. Electronic transitions due to nonbonding electrons carbonyl, aza-aromatic,and other compounds. Chem. Rev. 58 (4), 689–713.

Tan, Z., Fuchs, H., Lu, K., Hofzumahaus, A., Bohn, B., Broch, S., Dong, H., Gomm, S., Häseler, R., He, L., Holland, F., Li, X., Liu, Y., Lu, S., Rohrer, F., Shao, M., Wang, B., Wang, M., Wu, Y., Zeng, L., Zhang, Y., Wahner, A., Zhang, Y., 2017. Radical chemistry at a rural site (Wangdu) in the North China Plain: observation and model calculations of OH, HO2 and RO2 radicals. Atmos. Chem. Phys. 17 (1), 663–690.

Wang, Y., Guo, H., Zou, S., Lyu, X., Ling, Z., Cheng, H., Zeren, Y., 2018. Surface O3 photochemistry over the South China Sea: application of a near-explicit chemical mechanism box model. Environ. Pollut. 234, 155–166.

Wang, M., Xiang, X., Zuo, Y., Peng, J., Lu, K., Dempsey, C., Liu, P., Gao, S., 2020. Singlet oxygen production abilities of oxidated aromatic compounds in natural water. Chemosphere 258, 127308.

Weng, M.L., Zhu, L.Z., Yang, K., Chen, S.G., 2009. Levels and health risks of carbonyl compounds in selected public places in Hangzhou,China. J. Hazard. Mater. 164 (2–3), 700–706.

Woo, J.L., Kim, D.D., Schwier, A.N., Li, R., McNeill, V.F., 2013. Aqueous aerosol SOA formation: impact on aerosol physical properties. Faraday Discuss. 165, 357–367.

Xia, S.S., Eugene, A.J., Guzman, M.I., 2018. Cross photoreaction of glyoxylic and pyruvic acids in model aqueous aerosol. J. Phys. Chem. A 122 (31), 6457–6466.

Yamaji, M., Fujino, S., Horimoto, A., 2016. Photophysical and photochemical properties of an aromatic carbonyl compound for a moderate triplet energy sensitizer studied by steady state and laser flash photolysis. J. Photochem. Photobiol.A 317, 9–11.

Yang, X., Xue, L., Wang, T., Wang, X., Gao, J., Lee, S., Blake, D.R., Chai, F., Wang, W., 2018. Observations and explicit modeling of summertime carbonyl formation in Beijing: identification of key precursor species and their impact on atmospheric oxidation chemistry. J. Geophys. Res. Atmos. 123 (2), 1426–1440.

Yuan, B., Chen, W., Shao, M., Wang, M., Lu, S., Wang, B., Liu, Y., Chang, C.-C., Wang, B., 2012. Measurements of ambient hydrocarbons and carbonyls in the Pearl River Delta (PRD),China. Atmos. Res. 116, 93–104.

Zhang, R., Gen, M., Fu, T.M., Chan, C.K., 2021. Production of formate via oxidation of glyoxal promoted by particulate nitrate photolysis. Environ. Sci. Technol. 55 (9), 5711–5720.

Zhou, H., Yan, S., Lian, L., Song, W., 2019. Triplet-state photochemistry of dissolved organic matter: triplet-state energy distribution and surface electric charge conditions. Environ. Sci. Technol. 53 (5), 2482–2490.